holes from the valence-band edge to the reducing agent in solution as is shown in Figure 10a. Without propane in solution, of course, the photogenerated holes will attack solvents directly. Smaller CD factors for alkanes other than propane can be explained by their lower hole-capture cross sections or smaller overlap of their fluctuating energy levels with TiO_2 conduction-band edge.

It seems to be of interest to compare the results in this acid solvent with those in fluorosulfonic acid (HSO_3F), one of the superacids. In the latter solvent, alkanes are known to be oxidized at a diffusion-controlled rate on Pt at less anodic potential than the potential where solvent oxidation starts.[26,27] Therefore, the oxidation of alkanes in place of solvent oxidation is an exothermic reaction here. In addition, the oxidation is believed to involve the formation of an alkane radical which has a highly reducing ability. However, increase of photocurrents and any visually appreciable change were not found on the n-TiO_2 before and after the solvent was purged with methane, ethane, or propane.[28] This may imply no occurrence of an exothermic reaction in the superacid in accord with the result in triflic acid monohydrate.

A final problem to be discussed is a cause for a sizable anodic current flow, not associated with alkane oxidation, on the reverse-biased n-TiO_2 electrode in the dark. Clearly, avalanche breakdown of the material or Zener breakdown can be ruled out because the breakdown-produced holes should have the same fate as photogenerated holes. Instead, one possible path is an electron tunneling from the solvent, through a narrow space charge layer, into the conduction band as indicated in Figure 10b. A simple calculation using eq 2.22 in ref 18 with 10^{20} cm^{-3} for donor density and 100 for dielectric constant of the TiO_2 leads to a value of ca. 50 Å for the thickness of the space charge layer at 1.7 eV below the conduction-band edge when the electrode is biased at 4 V. The layer under the described condition appears to be somewhat thick for efficient electron tunneling to occur. It should be noted, however, that this estimate is made for the n-TiO_2 before the electrode treatment. If imperfections or energy levels in the bandgap in the bulk are generated in some fashion by the electrochemical or photoelectrochemical treatment of the TiO_2 in the strong acid at high temperatures, they may assist the electron transfer from a solvent molecule into the conduction band. The observed difference of corrosion behavior of the material can be explained by the proposed mechanisms for a charge transfer at the semiconductor–electrolyte interface on the illuminated n-TiO_2 (involving holes) and the reverse-biased n-TiO_2 in the dark (no holes generated to cause corrosion).

Registry No. TiO_2, 13463-67-7; propane, 74-98-6; triflic acid, 1493-13-6; methane, 74-82-8; ethane, 74-84-0; *n*-butane, 106-97-8; *n*-hexane, 110-54-3; methanol, 67-56-1.

(26) Bertram, J.; Coleman, J. P.; Fleischmann, M.; Pletcher, D. *J. Chem. Soc., Perkin Trans. 2* **1973**, 394.
(27) Coleman, J. P.; Pletcher, D. *J. Electroanal. Chem.* **1978**, *87*, 111.
(28) Harima, Y.; Morrison, S. R., unpublished work.

Nonionic Rodlike Micelles in Dilute and Semidilute Solutions: Intermicellar Interaction and the Scaling Law

Toyoko Imae

Department of Chemistry, Faculty of Science, Nagoya University, Chikusa, Nagoya 464, Japan
(Received: October 15, 1987; In Final Form: February 8, 1988)

The static and dynamic light scattering for aqueous NaCl solutions of heptaoxyethylene alkyl ethers (C_nE_7, n = 10, 12, 14, and 16) has been measured, and the characteristics of nonionic rodlike micelles have been analyzed at finite micelle concentrations, considering the micelle growth and the intermicellar interaction. While the second virial coefficient of rodlike micelles is small and scarcely depends on NaCl concentration and the alkyl chain length, the hydrodynamic virial coefficient is negative and the absolute values increase with an increase in micelle aggregation number, comparable to the increase of the friction coefficient. The solution behavior of rodlike micelles in dilute and semidilute regimes has been discussed on the basis of the scaling laws. The scaling laws obey to the relations with the characteristic exponent ν = 0.58–0.71. The deviation from the scaling laws was observed at higher micelle concentrations, suggesting the transition from the semidilute regime to the concentrated regime.

Introduction

The development of the laser light source and dynamic light scattering instrument has promoted the investigation of micelle size and shape. Especially, the simultaneous measurement of static and dynamic light scattering has been available to analyze the characteristics of large or rodlike micelles.

Young et al.[1] and Appell et al.[2,3] have measured the angular dissymmetry and the autocorrelation function from laser light scattering. They employed both quantities in order to distinguish between the possible shapes of large micelles formed at finite micelle concentrations[1-3] and estimated the flexibility of elongated rodlike micelles with the aid of the distinct experimental investigation.[2,3]

Candau et al.[4,5] have performed the intensity and correlation measurements for the light scattered from aqueous salt solutions of cationic surfactants within a concentration range from dilute to semidilute regimes. They have reported that the shape of micelles changes, depending on alkyl chain length and surfactant concentration,[4] and have first mentioned that the long flexible micelles entangle in the semidilute regime, obeying the scaling laws.[4,5]

The overlap or entanglement of rodlike micelles was first evidenced by Hoffmann et al. for aqueous solutions of tetradecylpyridinium *n*-heptanesulfonate[6] and cetylpyridinium salicylate.[7]

(1) Young, C. Y.; Missel, P. J.; Mazer, N. A.; Benedeck, G. B.; Carey, M. C. *J. Phys. Chem.* **1978**, *82*, 1375.
(2) Appell, J.; Porte, G. *J. Colloid Interface Sci.* **1981**, *81*, 85.
(3) Appell, J.; Porte, G.; Poggi, Y. *J. Colloid Interface Sci.* **1982**, *87*, 492.
(4) Candau, S. J.; Hirsh, E.; Zana, R. *J. Phys. (Les Ulis, Fr.)* **1984**, *45*, 1263.
(5) Candau, S. J.; Hirsh, E.; Zana, R. *J. Colloid Interface Sci.* **1985**, *105*, 521.
(6) Hoffmann, H.; Rehage, H.; Platz, G.; Schorr, W.; Thurn, H.; Ulbricht, W. *Colloid Polym. Sci.* **1982**, *260*, 1042.
(7) Hoffmann, H.; Platz, G.; Rehage, H.; Schorr, W. *Adv. Colloid Interface Sci.* **1982**, *17*, 275.

0022-3654/88/2092-5721$01.50/0

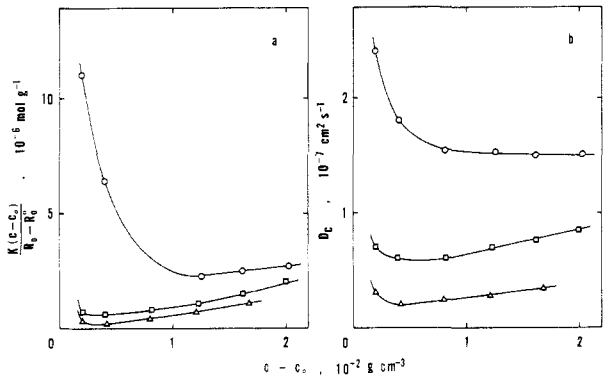

Figure 1. Debye plots and diffusion coefficients at zero scattering angle for aqueous NaCl solutions of $C_{14}E_7$ at 25 °C. (a) Debye plot; (b) diffusion coefficient. NaCl concentration (M): ○, 1; □, 2; △, 3.

Imae et al.[8-10] have measured the static light scattering for aqueous salt solutions of alkyltrimethylammonium halides. The threshold micelle concentration of overlap was evaluated,[8-10] and the scaling laws for rodlike micelles in dilute and semidilute regimes were discussed.[9,10]

The application of the scaling laws to the entanglement of elongated nonionic micelles was carried out by Kato et al.[11]

Recently, Zhou et al.[12] have examined the rotational diffusion coefficient for a polar organic solution of metal soap and discussed the reological behavior of rodlike micelles in the semidilute regime.

For the investigation at finite micelle concentrations where large or rodlike micelles are formed, generally, the intermicellar interaction should be taken into account, besides the micelle growth. Nevertheless, no literature discusses simultaneously both effects at finite concentrations, because that the separation of two effects is difficult.

In this paper, static and dynamic light scattering is measured for aqueous NaCl solutions of C_nE_7, and the analysis for the characteristics of rodlike micelles at finite micelle concentrations is reported. The analysis includes two contributions of micelle size and intermicellar interaction, which depend on micelle concentration. Moreover, the light scattering data in dilute and semidilute regimes is analyzed and the characteristic exponent of scaling laws is evaluated.

Experimental Section

Samples of C_nE_7 were purchased from Nikko Chemicals Co., Ltd. (Tokyo). NaCl was ignited for 1 h, and water was redistilled from alkaline $KMnO_4$.

The measurement of specific refractive index increment was carried out on Otsuka Denshi differential refractometer RM-102 and performed at a 488-nm wavelength and 25 °C.

The static and dynamic light scattering was measured on Otsuka Denshi dynamic light scattering spectrophotometer DLS-700. The light source is an argon ion laser of a 488-nm wavelength. The scattering angle was changed from 20° to 150°. The cell housing was filled with di-*n*-butyl phthalate and kept at 25 °C. Solvents and solutions were purified by filtering them through a Millipore membrane filter. The procedure of static light scattering has been described in detail elsewhere.[9]

On dynamic light scattering, the second-order autocorrelation function measured in homodyne mode was computer-analyzed in order to provide the first-order normalized electron field correlation function $g^1(\tau)$. The mean characteristic line width $\bar{\Gamma}$ was evaluated by the cumulant method. Then the diffusion coefficient D can be calculated by the relation of $D = \bar{\Gamma}/\mu^2$, where μ is the magnitude of scattering vector.

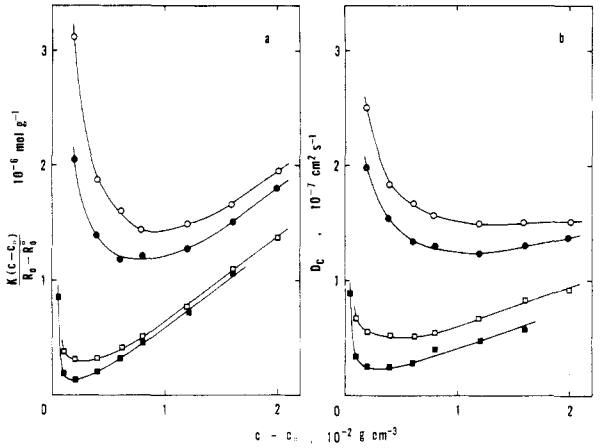

Figure 2. Debye plots and diffusion coefficients at zero scattering angle for aqueous NaCl solutions of $C_{16}E_7$ at 25 °C. (a) Debye plot; (b) diffusion coefficient. NaCl concentration (M): ○, 0; ●, 0.1; □, 1; ■, 2.

Results

The results of static and dynamic light scattering measurements for aqueous NaCl solutions of $C_{14}E_7$ and $C_{16}E_7$ are extrapolated to the zero scattering angle and are shown as a function of micelle concentration $c - c_0$ in Figures 1 and 2. The Debye plots and the diffusion coefficients decrease abruptly at low micelle concentrations and increase through a minimum at high micelle concentrations. The minimum values shift to lower micelle concentration with an increase in NaCl concentration and in the alkyl chain length. A similar feature was also observed for $C_{10}E_7$ in 3 and 4 M NaCl and for $C_{12}E_7$ in 2, 3, 3.5, and 4 M NaCl.

The Debye plot at the angle θ for dilute aqueous solutions of micelles may be described by

$$K(c - c_0)/(R_\theta - R_\theta^0) = (1/M_{app})(1 + \tfrac{1}{3}R_{G,app}{}^2\mu^2) \quad (1)$$

for small $R_{G,app}{}^2\mu^2$, and the diffusion coefficient for 0° direction can be written as

$$D_c = k_B T/6\pi\eta_0 R_{H,app} \quad (2)$$

where K is the optical constant and R and R^0 are the reduced scattering intensities at the surfactant concentration c and the critical micelle concentration c_0, respectively. M, R_G, and R_H are the molecular weight, radius of gyration, and hydrodynamic redius of micelles, respectively, and the subscript app means that the values are apparent. k_B is the Boltzmann constant, T is the absolute temperature, and η_0 is the viscosity of solvent.

After the values of $K(c - c_0)/(R_\theta - R_\theta^0)$ and D were plotted against μ^2, the values of M_{app}, $R_{G,app}$, and $R_{H,app}$ were evaluated from the extrapolation to the zero angle or from the slope of the initial straight line. Table I gives the apparent molecular weight, radius of gyration, and the hydrodynamic radius obtained for aqueous NaCl solutions of C_nE_7 at the micelle concentration, where the Debye plot takes the minimum value and the micelles with the maximum molecular weight should be formed. These apparent values enlarge at high NaCl concentrations and for surfactants with long alkyl chain.

Table I also includes the values of specific refractive index increment $(\partial\tilde{n}/\partial c)_{C_s}$ at constant salt concentration C_s (M) and apparent micelle aggregation number $m_{app} = M_{app}/M_1$, where $\tilde{n}$ is the refractive index of solution and M_1 is a molecular weight of surfactant molecule. The large micelle aggregation number such as indicated in Table I implies the formation of rodlike micelles.

Discussion

Characteristics of Rodlike Micelles. If the intermicellar interaction is not considered, (1) and (2) would give the characteristics for micelles formed at a certain micelle concentration. However, the intermicellar interaction, besides the micelle growth, should be taken into consideration at the finite micelle concentration. Then the light scattered at the angle θ from dilute aqueous

(8) Imae, T.; Kamiya, R.; Ikeda, S. *J. Colloid Interface Sci.* **1985**, *108*, 215.
(9) Imae, T.; Ikeda, S. *J. Phys. Chem.* **1986**, *90*, 5216.
(10) Imae, T.; Ikeda, S. *Colloid Polym. Sci.* **1987**, *265*, 1090.
(11) Kato, T.; Anzai, S.; Seimiya, T. *J. Phys. Chem.* **1987**, *91*, 4655.
(12) Zhou, Z.; Georgalis, Y.; Llang, W.; Li, J.; Xu, R.; Chu, B. *J. Colloid Interface Sci.* **1987**, *116*, 473.

TABLE I: Characteristics of Rodlike Micelles of Heptaoxyethylene Alkyl Ethers in Aqueous NaCl Solutions at 25 °C

	C_s, M	$(\partial\tilde{n}/\partial c)_{C_s}$, cm^3 g^{-1}	$10^{-4}M_{app}$, g mol^{-1}	m_{app}	$R_{G,app}$, nm	$R_{H,app}$, nm	ρ_{app}
$C_{10}E_7$	3	0.096_7	10.8	232		6.8	
	4	0.085_6	39.9	855		14.2	
$C_{12}E_7$	2	0.129	21.5	435		10.1	
	3	0.128	63.1	1270	33.5	22.6	1.48
	3.5	0.117[a]	108	2190	42.8	33.0	1.30
	4	0.095_7	1300	26300	134	131	1.02
$C_{14}E_7$	1	0.134[a]	44.1	844	24.4	14.9	1.64
	2	0.131	165	3160	55.0	34.5	1.59
	3	0.128	443	8480	95.7	94.3	1.01
$C_{16}E_7$	0	0.138	69.4	1260	26.3	15.7	1.68
	0.1	0.138	84.9	1540	31.1	17.9	1.74
	1	0.132	320	5810	69.0	40.4	1.71
	2	0.129	773	14000	135	82.1	1.64

[a] Interpolated values.

TABLE II: Characteristics of Rodlike Micelles of Heptaoxyethylene Alkyl Ethers in Aqueous NaCl Solutions at 25 °C (with a Parameter of A = 2/15)

	C_s, M	$10^{-4}M$, g mol^{-1}	m	R_G, nm	R_H, nm	ρ	10^5B_2, mol cm^3 g^{-2}	$10^5B_{2,rod}$, mol cm^3 g^{-2}	k_f, cm^3 g^{-1}	k_D, cm^3 g^{-1}	$10^2(c-c_0)^*$, g cm^{-3}
$C_{12}E_7$	3.5	109	2200	42.9	31.8	1.35	0.02	5.28	4.0	−4.5	0.29–0.55
	4	1450	29400	142	95.1	1.49	0.05	0.33	48.0	−34.2	0.11–0.20
$C_{14}E_7$	1	54.1	1040	27.1	13.7	1.97	1.65	10.2	23.5	−6.6	0.57–1.08
	2	170	3240	55.8	32.6	1.71	0.20	4.39	20.1	−14.2	0.20–0.39
	3	661	12600	117	69.2	1.69	0.89	1.28	181	−64.1	0.08–0.16
$C_{16}E_7$	0	78.8	1430	28.0	14.9	1.87	1.08	5.86	21.9	−5.8	0.74–1.42
	0.1	92.1	1670	32.4	17.0	1.90	0.77	5.76	21.0	−7.7	0.57–1.08
	1	327	5930	69.7	39.2	1.78	0.16	2.11	25.4	−15.2	0.20–0.38
	2	811	14700	138	75.3	1.84	0.15	1.35	63.9	−40.8	0.06–0.12

TABLE III: Characteristics of Rodlike Micelles of Heptaoxyethylene Alkyl Ethers in Aqueous NaCl Solutions at 25 °C (with a Parameter of A = 13/75)

	C_s, M	10^{-4}M, g mol^{-1}	m	R_G, nm	R_H, nm	ρ	10^5B_2, mol cm^3 g^{-2}	$10^5B_{2,rod}$, mol cm^3 g^{-2}	k_f, cm^3 g^{-1}	k_D, cm^3 g^{-1}	$10^2(c-c_0)^*$, g cm^{-3}
$C_{12}E_7$	3.5	83.7	1690	37.6	16.5	2.27	−1.73	6.87	33.7	−63.6	0.33–0.62
	4	1120	22600	124	68.2	1.82	−0.08	0.42	41.8	−60.0	0.15–0.29
$C_{14}E_7$	1	41.6	796	23.7	12.1	1.96	−0.54	13.2	9.1	−14.5	0.64–1.23
	2	130	2490	48.9	19.9	2.45	−2.04	5.78	52.7	−107	0.23–0.44
	3	509	9730	102	71.8	1.43	0.35	1.64	91.9	−57.4	0.10–0.19
$C_{16}E_7$	0	60.6	1100	24.6	11.4	2.16	−1.32	7.67	17.5	−34.4	0.85–1.62
	0.1	70.8	1290	28.4	12.1	2.35	−1.95	7.48	25.3	−53.9	0.64–1.23
	1	251	4560	61.2	24.7	2.48	−2.14	2.75	83.7	−195	0.23–0.44
	2	624	11300	121	47.7	2.54	−0.75	1.74	109.4	−204	0.07–0.14

solutions of rodlike micelles includes the contribution of the virial coefficient, in addition to the contribution of particle scattering factor. Therefore, for small $R_G^2\mu^2$

$$K(c-c_0)/(R_\theta - R_\theta^0) = (1/M)(1 + \tfrac{1}{3}R_G^2\mu^2) + 2B_2(c-c_0) \quad (3)$$

$$D = D_c[1 + AR_G^2\mu^2] \quad (4)$$

$$D_c = D_0[1 + k_D(c-c_0)] \quad (5)$$

and

$$D_0 = k_B T/6\pi\eta_0 R_H \quad (6)$$

instead of (1) and (2), where B_2 is the second virial coefficient and k_D is the hydrodynamic virial coefficient.

The value of coefficient A is given as 2/15 or 13/75 for linear chain.[13,14] The hydrodynamic virial coefficient k_D can be written as[15]

$$k_D = 2B_2M - k_f - \bar{v} \quad (7)$$

and the relation

$$k_f = (k_BT/\eta_0)(B_2^2N_AM/12\pi^2)^{1/3}/D_0 \quad (8)$$

is proposed for the friction coefficient of rod particle.[16] $\bar{v}$ is the partial specific volume of a particle, and N_A is Avogadro's number.

From the plot of D against μ^2, the values of D_c and R_G can be obtained from (4). Using the R_G value and from the plot of $K(c-c_0)/(R_\theta - R_\theta^0)$ against μ^2, the values of M and B_2 are evaluated, according to (3). When the $\bar{v}$ value of 0.965 cm^3 g^{-1} is taken from literature,[17] the value of D_0 is obtained from (5), (7), and (8) and then the values of k_f, k_D and R_H can be evaluated. The values obtained with A = 2/15 or 13/75 for the micelle solutions at the minimum of Debye plot are summarized in Tables II and III, where the micelle aggregation number m is also included.

The aggregation number, radius of gyration, and hydrodynamic radius of rodlike micelles increase with an increase in NaCl concentration and the alkyl chain length. The values for A = 2/15 are generally larger than those for A = 13/75.

The second virial coefficient of rodlike micelles scarcely depends on NaCl concentration and the alkyl chain length, and the values are rather small and below $\pm 2 \times 10^{-5}$ mol cm^3 g^{-2}. The B_2 values for A = 2/15 are positive, while those for A = 13/75 are negative.

If only the steric repulsive forces between the rigid rod particle cores contributes to the second virial coefficient, without van der

(13) Burchard, W.; Schmidt, M.; Stockmayer, W. H. *Macromolecules* **1980**, *13*, 580.
(14) Burchard, W. *Adv. Polym. Sci.* **1983**, *48*, 1.
(15) Yamakawa, H. *Modern Theory of Polymer Solution*; Harper and Row: New York, 1971; p 181.
(16) Kubota, K.; Tominaga, Y.; Fujime, S. *Macromolecules* **1986**, *19*, 1604.
(17) Güveli, D. E.; Davis, S. S.; Kayes, J. B. *J. Colloid Interface Sci.* **1983**, *91*, 1.

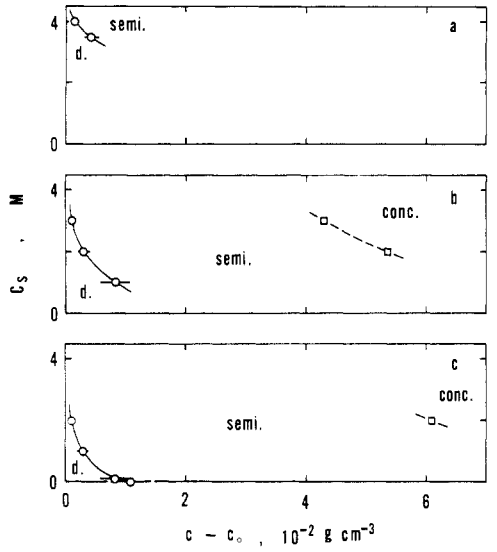

Figure 3. Diagrams of dilute, semidilute, and concentrated regimes as a function of NaCl concentration. (a) $C_{12}E_7$; (b) $C_{14}E_7$; (c) $C_{16}E_7$. O, the threshold micelle concentration of overlap; □, the micelle concentration for the transition from semidilute to concentrated regime.

Waals attractive interaction forces, the second virial coefficient for rigid rod particle[18] can be rewritten as

$$B_{2,\mathrm{rod}} = 6\pi N_A r R_G^2 / M^2 \quad (9)$$

utilizing the relation of $R_G^2 = L^2/12$, where r and L are the radius and the contour length of a rigid rod, respectively. Now only the repulsive interaction forces from the intermicellar excluded volume are considered but the electrostatic repulsion forces is not, because micelles of nonionic surfactants are concerned in this work.

When the r values of 3.0, 3.6, and 4.1 nm are adopted for rodlike micelles of $C_{12}E_7$, $C_{14}E_7$, and $C_{16}E_7$, respectively, the values of $B_{2,\mathrm{rod}}$ can be calculated, as listed in Tables II and III. The second virial coefficient evaluated from the observed light scattering data is less than the values for rods which take into account the steric repulsion only. This indicates that the steric repulsion of rodlike micelles should be balanced by van der Waals attraction between them. Then, for dilute aqueous solutions of rodlike micelles, the change of micelle size rather than the intermicellar interaction mainly contributes to the Debye plot.

The friction coefficient of rodlike micelles strongly depends on micelle molecular weight, as assumed from (8), and changes from 4 to 180 cm^3 g^{-1}. The value of hydrodynamic virial coefficient of rodlike micelles is negative and ranges between −5 and −200 cm^3 g^{-1}, comparable to the absolute value of the friction coefficient. This suggests the strong contribution of the friction coefficient to the hydrodynamic virial coefficient. Therefore, it is concluded that the decrease of the diffusion coefficient with increasing micelle concentration is due to the hydrodynamic interaction, besides the micellar growth, and the contribution is stronger for rodlike micelles with higher molecular weight.

A dimensionless quantity $\rho = R_G/R_H$ defined by the ratio of the radius of gyration to the hydrodynamic radius is a valuable parameter associated with the flexibility of linear chains. For flexible linear polymers, the theoretical values of 1.504 and 1.479[19] at the θ temperature and the experimental values of 1.27,[20] 1.28,[19] and 1.38–1.66[21] have been reported. Recently, Kubota et al.[16] proposed the ρ values of 2.88 or 2.94 for poly(γ-benzyl L-glutamate), which is a fairly rigid rod.

The ρ values for rodlike micelles of C_nE_7 are calculated and listed in Tables I–III. The averaged values of 1.4_8, 1.7_3, and 2.1_6, respectively, were obtained, independent of NaCl concentration

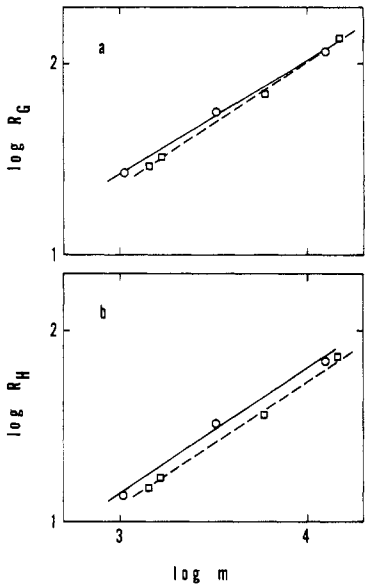

Figure 4. Double-logarithmic plots of the radius of gyration and the hydrodynamic radius of rodlike micelles of C_nE_7 against the micelle aggregation number. The values were taken from Table II. (a) Radius of gyration; (b) hydrodynamic radius. O, $C_{14}E_7$; □, $C_{16}E_7$.

and the alkyl chain length or micelle aggregation number. These values are located in between ones for flexible chains and a fairly rigid rod.

Semidilute Solutions and the Scaling Law. When the micelle concentration is increased, rodlike micelles overlap and entangle with one another.[4-12] The threshold micelle concentration of overlap is defined by[22]

$$M/[(2R_G)^3 N_A] \approx (c - c_0)^* \approx M/[(4/3)\pi R_G^3 N_A] \quad (10)$$

As seen in Tables II and III and Figure 3, the overlap threshold values for rodlike micelles of C_nE_7 decrease with an increase in NaCl concentration and the alkyl chain length.

The solutions of rodlike micelles can be divided into two regions distinguished by this characteristic micelle concentration, that is, dilute and semidilute regimes. The solution properties in each regime may be described by the scaling laws as similar as those for isolated and entangled polymer chains.[23]

For the dilute solutions where micelles isolate without any contact with one another, the radius of gyration and the hydrodynamic radius of micelles are scaled for the micelle aggregation number by the relations of

$$R_G \sim m^{\nu_G} \quad (11)$$

and

$$D_0^{-1} \sim R_H \sim m^{\nu_H} \quad (12)$$

In the semidilute regime, rodlike micelles entangle together and form a network which is characterized by the correlation length ξ of a blob, i.e., a unit of mesh of a network. If the m_ξ, ξ_G, and ξ_H represent the aggregation number, the static correlation length, and the hydrodynamic correlation length of blobs, respectively, the scaling laws against micelle concentrations in semidilute regime can be written as

$$K(c - c_0)/(R_0 - R_0^0) \sim m_\xi^{-1} \sim \xi_G^{-1/\nu_G} \sim (c - c_0)^{1/(3\nu_G - 1)} \quad (13)$$

and

$$D_c \sim \xi_H^{-1} \sim (c - c_0)^{\nu_H/(3\nu_H - 1)} \quad (14)$$

Figure 4 illustrates the double-logarithmic plots of R_G and R_H against m for data from Table II. The linear relation is realized

(18) Zimm, B. H. *J. Chem. Phys.* **1946**, *14*, 164.
(19) Tsunashima, Y.; Nemoto, N.; Kurata, M. *Macromolecules* **1983**, *16*, 1184.
(20) Schmidt, M.; Burchard, W. *Macromolecules* **1981**, *14*, 210.
(21) Kato, T.; Katsuki, T.; Takahashi, A. *Macromolecules* **1984**, *17*, 1726.
(22) Cotton, J. P.; Nierlich, M.; Boue, F.; Daoud, M.; Farnoux, B.; Jannink, G.; Duplessix, R.; Picot, C. *J. Chem. Phys.* **1976**, *65*, 1101.
(23) de Gennes, P. G. *Scaling Concepts in Polymer Physics*; Cornell University: Ithaca, London, 1979.

TABLE IV: Scaling Law for Aqueous NaCl Solutions of Heptaoxyethylene Alkyl Ethers at 25 °C

	ν_G (eq 11)			ν_H (eq 12)		
	I[a]	II	III	I	II	III
$C_{14}E_7$	0.58	0.59	0.58	0.71	0.65	0.69
$C_{16}E_7$	0.65	0.64	0.66	0.63	0.65	0.59

	C_s, M	ν_G (eq 13)	ν_H (eq 14)
$C_{14}E_7$	2	0.60	0.69
	3	0.58	0.54
$C_{16}E_7$	1	0.62	0.79
	2	0.61	0.62

[a] Data from Tables I, II, and III were used for methods I, II, and III, respectively.

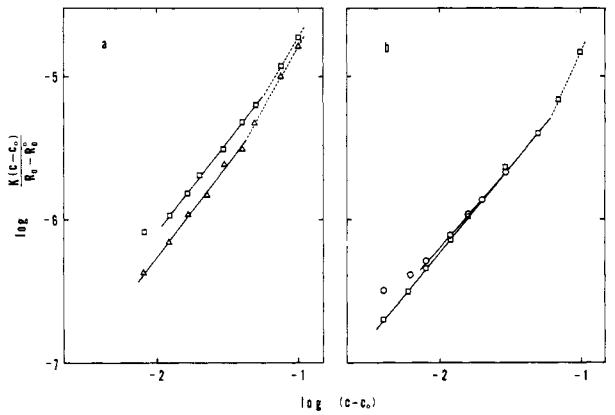

Figure 5. Double-logarithmic plots of the reciprocal scattering intensity against micelle concentration for semidilute solutions of C_nE_7. (a) $C_{14}E_7$; (b) $C_{16}E_7$. NaCl concentration (M): ○, 1; □, 2; △, 3.

for each system. The obtained ν values are listed in Table IV, where the ν values for data from Tables I and III are also included.

The light scattering data for semidilute micelle solutions were plotted according to the scaling laws of (13) and (14). Figures 5 and 6 show the double-logarithmic plots of the reciprocal scattering intensity and the diffusion coefficient, respectively, against micelle concentrations for aqueous NaCl solutions of $C_{14}E_7$ and $C_{16}E_7$. The ν values in (13) and (14) are evaluated from the slope of the straight lines in Figures 4 and 5 and listed in Table IV.

The ν values for $C_{14}E_7$ and $C_{16}E_7$ in dilute solutions range between 0.58 and 0.71 and do not depend on whether the correction of intermicellar interaction is carried out on the evaluation of micelle parameters or not. The ν values for semidilute regime are averaged to 0.63, which is within the limits of the ν values for the dilute regime.

The ν values for dilute and semidilute solutions are independent of NaCl concentration and the alkyl chain length, and the ν values for static light scattering are consistent with those for dynamic light scattering. It can be manifested that the solution properties for micelles and blobs of $C_{14}E_7$ and $C_{16}E_7$ are described by the scaling laws with same characteristic exponent.

The static light scattering for aqueous salt solutions of alkyltrimethylammonium halides[9,10] and dimethyloleylamine oxide[24] has been measured, and the ν_G values for rodlike micelles were reported. The ν_G values of 0.54–0.55 for alkyltrimethylammonium halides are smaller than those for C_nE_7, and the value of 0.70 for dimethyloleylamine oxide is larger than those. This may suggest the difference of the flexibility for rodlike micelles of these surfactants.

As seen in Figure 5, the values of reciprocal scattering intensity obtained at high micelle concentrations for $C_{14}E_7$ in 2 and 3 M NaCl and for $C_{16}E_7$ in 2 M NaCl deviate from the straight line for the scaling law in (13), although the same behavior is not clear for the scaling law in (14) which is shown in Figure 6. The threshold micelle concentration of the deviation was obtained as

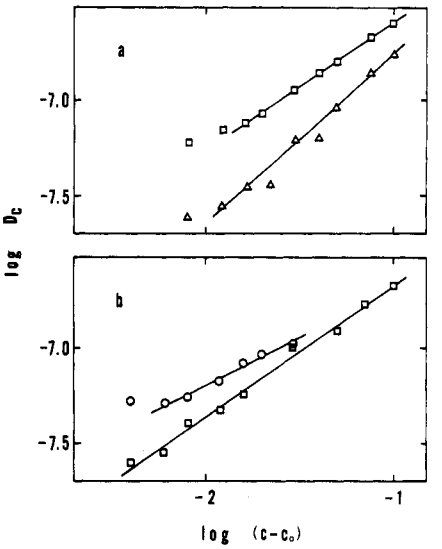

Figure 6. Double-logarithmic plots of the diffusion coefficient against micelle concentration for semidilute solutions of C_nE_7. (a) $C_{14}E_7$; (b) $C_{16}E_7$. NaCl concentration (M): ○, 1; □, 2; △, 3.

5.6 and 4.3 × 10^{-2} g cm^{-3} for $C_{14}E_7$ in 2 and 3 M NaCl, respectively, and 6.1 × 10^{-2} g cm^{-3} for $C_{16}E_7$ in 2 M NaCl. These threshold values are 1 to 2 orders of magnitude higher than the threshold micelle concentration of overlap and seem to be almost independent of the alkyl chain length. The micelle concentrations above the threshold value of deviation may be assigned to the concentrated regime but not to the semidilute regime.

The boundary between the semidilute and concentrated regimes for randomly coiled polymer chains has been discussed by Graessley,[25] and the theoretical estimation of the crossover concentration was developed for polymer chains with different rigidity from random coils to rigid rods.[26] Recently it has been reported for polymer solutions that there is the obvious transition in plots of scattering intensity and diffusion coefficient against the polymer concentration, indicating the transition from the semidilute to concentrated regime.[27]

Aqueous solutions of oligooxyethylene alkyl ethers separate into two liquid phases above the lower consolute temperature or the cloud point, T_c, and the addition of NaCl to aqueous solutions of C_nE_7 decreases the lower consolute temperature.[28] On the other hand, in the vicinity of the lower consolute boundary, the importance of concentration fluctuations on light scattering was debated for aqueous solutions of oligooxyethylene alkyl ethers in the past few years,[11,29-36] and the temperature regime for critical concentration fluctuations was presented as $(T_c - 4\ °C) < T < T_c$ by Wilcoxon and Kaler.[36]

Such a temperature regime is completely applied to a 4 M NaCl solution of $C_{12}E_7$ at 25 °C in the present work, and the micelle aggregation number obtained for this solution may be overestimated. We will report elsewhere the effect of temperature on light scattering for aqueous solutions of surfactants, in relation to the liquid–liquid phase separation.

In addition, the solution properties of rodlike micelles in dilute and semidilute regimes remarkably change even in the rheological behavior. We will demonstrate in a following paper that the

(24) Imae, T.; Ikeda, S. *Colloid Polym. Sci.* **1985**, *263*, 756.
(25) Graessley, W. W. *Polymer* **1980**, *21*, 258.
(26) Ying, Q.; Chu, B. *Macromolecules* **1987**, *20*, 362.
(27) Ying, Q.; Chu, B. *Macromolecules* **1987**, *20*, 871.
(28) Imae, T.; Sasaki, M.; Abe, A.; Ikeda, S. *Langmuir* **1988**, *4*, 414.
(29) Hayter, J. B.; Zulauf, M. *Colloid Polym. Sci.* **1982**, *260*, 1023.
(30) Zulauf, M.; Rosenbusch, J. P. *J. Phys. Chem.* **1983**, *87*, 856.
(31) Nilsson, P.-G.; Wennerström, H.; Lindman, B. *J. Phys. Chem.* **1983**, *87*, 1377.
(32) Corti, M.; Minero, C.; Degiorgio, V. *J. Phys. Chem.* **1984**, *88*, 309.
(33) Zulauf, M.; Weckström, K.; Hayter, J. B.; Degiorgio, V.; Corti, M. *J. Phys. Chem.* **1985**, *89*, 3411.
(34) Zana, R.; Weill, C. *J. Phys., Lett.* **1985**, *46*, L-953.
(35) Kato, T.; Seimiya, T. *J. Phys. Chem.* **1986**, *90*, 3159.
(36) Wilcoxon, J. P.; Kaler, E. W. *J. Chem. Phys.* **1987**, *86*, 4684.

rheological investigation for aqueous C_nE_7 solutions can confirm the results from light scattering.[37]

Conclusion

In this work, the measurement of laser light scattering was carried out for aqueous NaCl solutions of C_nE_7. Moreover, the size and mutual interaction of rodlike micelles in dilute regime were analyzed at a finite micelle concentration, and the properties of the entangled micelles in dilute and semidilute regimes were examined on the basis of the scaling laws. Several important conclusions were obtained:

(1) The Debye plots and the diffusion coefficients exhibit minimum values around the threshold micelle concentration of overlap, above which micelles entangle together.

(2) Whereas the threshold micelle concentrations of overlap decrease with an increase in NaCl concentration and the alkyl chain length, the aggregation number, radius of gyration, and hydrodynamic radius of rodlike micelles increase with them.

(3) While the second virial coefficient of rodlike micelles is small and scarcely depends on micelle aggregation number, the friction coefficient remarkably increases with micelle size and strongly contributes to the hydrodynamic virial coefficient, resulting a negative large virial value.

(4) When a value of 13/75 is applied instead of 2/15 for the coefficient A on angular dependence of diffusion coefficient, the numerical values of the second virial coefficient change from positive to negative.

(5) The characteristic exponent ν for several scaling laws associated with light scattering experiments in dilute and semidilute regimes ranges between 0.58 and 0.71, in general, independent of NaCl concentration and the alkyl chain length. Moreover, the ν values from static and dynamic light scattering are consistent with each other.

(6) The ν values increase in the order of alkyltrimethylammonium halides < C_nE_7 < dimethyloleylamine oxide, reflecting the difference of the flexibility of rodlike micelles.

(7) The deviation from the straight line on the scaling laws was observed at micelle concentrations higher than 10–100 times the threshold value of overlap, suggesting the transition from the semidilute regime to the concentrated regime.

Acknowledgment. I acknowledge Professor Shoichi Ikeda for valuable suggestions.

Registry No. $C_{10}E_7$, 39840-09-0; $C_{12}E_7$, 3055-97-8; $C_{14}E_7$, 40036-79-1; $C_{16}E_7$, 4486-31-1; NaCl, 7647-14-5.

(37) Imae, T.; Sasaki, M.; Ikeda, S. *J. Colloid Interface Sci.*, in press.

Kinetic Studies in Heterogeneous Photocatalysis. 1. Photocatalytic Degradation of Chlorinated Phenols in Aerated Aqueous Solutions over TiO_2 Supported on a Glass Matrix

Hussain Al-Ekabi and Nick Serpone*

Department of Chemistry, Concordia University, 1455 de Maisonneuve Blvd. West, Montreal, Quebec, Canada H3G-1M8 *(Received: October 22, 1987; In Final Form: April 25, 1988)*

The photocatalytic degradation of phenol, 4-chlorophenol, 2,4-dichlorophenol, and 2,4,5-trichlorophenol over TiO_2 (anatase) has been investigated by using three photochemical reactors. TiO_2 was used as a thin film, coating the internal surface of a glass coil (reactors I and II) or the external surface of glass beads (reactor III). The degradation of the four phenolic compounds, in a continuous recirculation mode in all three reactors, approximates first-order kinetics to near-complete degradation. The Langmuir–Hinshelwood kinetics have been modified slightly to rationalize the first-order behavior in solid–liquid reactions and to argue in favor of a surface reaction; the degradation reactions occur on the TiO_2 particle surface. In the multipass mode experiments, both reactors I and II exhibit higher degradation rates for phenol at the higher flow rates. By contrast, the greater degradation is associated with the lower flow rates in the single-pass mode experiments.

Introduction

The presence of chlorinated hydrocarbons and other organic contaminants in drinking waters in North America[1,2] and Europe[3] can have serious consequences on human health and on the quality of the environment.[4] The widespread utilization of chlorinated aromatic compounds as pesticides and herbicides is attracting increased concern. The degradation of these compounds is possible via chemical, photochemical, and biological processes,[4] but most of these require long treatment periods and in practice are often difficult to apply in the disposal of wastes.

The photocatalytic mineralization of chlorinated hydrocarbons and other organic contaminants in water mediated by illuminated TiO_2 has been demonstrated.[5-8] TiO_2 dispersions and conventional

(1) Symons, J. M.; Bellor, T. A.; Carswell, J. K.; De Marco, J.; Kropp, K. L.; Robeck, G. G.; Seeger, D. R.; Slocum, C. J.; Smith, B. L.; Stevens, A. A. *J.—Am. Water Works Assoc.* **1975**, *67*, 634.

(2) Foley, P. D.; Missingham, G. A. *J.—Am. Water Works Assoc.* **1976**, *68*, 105.

(3) Rook, J. J. *J.—Am. Water Works Assoc.* **1976**, *68*, 168.

(4) Hutzinger, O., Ed. *The Handbook of Environmental Chemistry*; Springer-Verlag: Berlin, 1982.

(5) (a) Hsiao, C.-Y.; Lee, C.-L.; Ollis, D. F. *J. Catal.* **1983**, *82*, 418. (b) Pruden, A. L.; Ollis, D. F. *Environ. Sci. Technol.* **1983**, *17*, 628. (c) Pruden, A. L.; Ollis, D. F. *J. Catal.* **1983**, *82*, 404. (d) Ollis, D. F.; Hsiao, C.-Y.; Budiman, L.; Lee, C.-L. *J. Catal.* **1984**, *88*, 89. (e) Nguyen, T.; Ollis, D. F. *J. Phys. Chem.* **1984**, *88*, 3386. (f) Ollis, D. F. *Environ. Sci. Technol.* **1985**, *19*, 480.

(6) (a) Matthews, R. W. *J. Chem. Soc., Faraday Trans. 1* **1984**, *80*, 457. (b) Matthews, R. W. *J. Catal.* **1986**, *97*, 565. (c) Matthews, R. W. *Water Res.* **1986**, *20*, 569. (d) Matthews, R. W. *J. Phys. Chem.* **1987**, *91*, 3328. (e) Matthews, R. W. *Sol. Energy* **1987**, *38*, 405. (f) Matthews, R. W. *Aust. J. Chem.* **1987**, *40*, 667.

(7) Okamoto, K.; Yamamoto, Y.; Tanaka, H.; Tanaka, M. *Bull. Chem. Soc. Jpn.* **1985**, *58*, 2015.

0022-3654/88/2092-5726$01.50/0